

Multimode Cepheids in the Large Magellanic Cloud - challenges for theory

W.A. Dziembowski^{*,†} and R. Smolec[†]

^{*}Warsaw University Observatory, Al. Ujazdowskie 4, 00-478 Warsaw, Poland

[†]Copernicus Astronomical Center, ul. Bartycka 18, 00-716 Warsaw, Poland

Abstract. Data on multimode Cepheids from OGLE-III catalog of the LMC Cepheids are confronted with results from model calculations. Models whose radial mode periods are consistent with observation are not always in agreement with published evolutionary models. Nonradial mode interpretation is considered for the cases of unusual period ratios. The greatest challenge for stellar pulsation theory is explanation of double-mode pulsators with period ratios near 0.6.

Keywords: Cepheids – stars: oscillations – stars: evolution – Magellanic Clouds

PACS: 97.10.Sj, 97.30.Gj

INTRODUCTION

The OGLE-III catalog of the LMC Cepheids [1] contains a large number of objects with more than one mode excited. There are 61 classical beat Cepheids pulsating in the fundamental and first overtone modes (F/1O) and 203 objects pulsating in the first two overtones (1O/2O). The rare types of multimode radial pulsators include two 1O/3O objects, two triple-mode pulsators of the F/1O/2O type and three of the 1O/2O/3O type [2]. Of these rare Cepheids, only two 1O/2O/3O objects were known before [3]. More common (29 objects) are first overtone pulsators with additional periods which are equal about 0.6 of the dominant ones and cannot be explained in terms of radial overtones. We denote them as the 1O/X pulsators. In Figure 1, we show period distribution of various types of short period Cepheids.

In a number of LMC Cepheids, additional periods close to the dominant modes are detected. These were found in a relatively small fraction (4%) of fundamental mode Cepheids but in a significant fraction of objects with excited overtones (e.g. 18% in 1O and 36% in 1O/2O).

INFERENCE FROM DATA ON TWO RADIAL MODE PERIODS AND W_I

Most of multimode pulsators are found among short-period Cepheids, which, as first noted in [4] and [5], are not well explained in terms of evolutionary models of core-helium burning stars (second and third crossings of the instability strip). Some of them may be in the first crossing phase, which is much faster, but there are also problems with this interpretation.

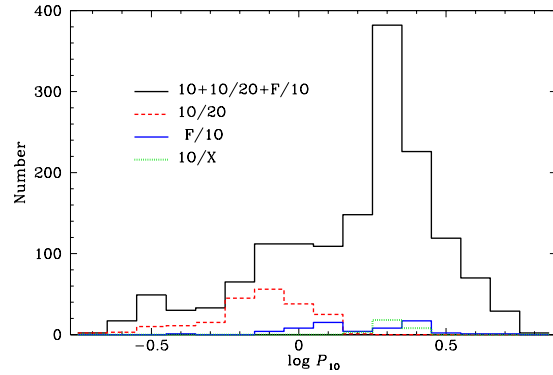


FIGURE 1. Period distribution for the LMC Cepheids with the first overtone excited. The 1O/2O pulsators constitute 13.8% of the sample but dominate in a certain period range. The F/1O pulsators constitute only 4.1%. The 1O/X objects (1.9% of the sample) and the long-period F/1O pulsators occur in the same period range.

Data on two periods of radial modes and on Wesenheit indexes, such as shown in Figures 2 and 3, yield strong constraints on stellar models. In principle, color data may also be used but they are less accurate. Instead, as a constraint on effective temperatures, a requirement of mode instability was adopted in recent works exploiting data on multimode Cepheids ([6], [7], [8] and [9], hereafter DS). In DS, which was devoted almost exclusively to the 1O/2O LMC Cepheids, the W_I and period data (Figure 3) were used to constrain parameters of these objects, in particular, their masses.

In DS and here, model values of W_I were obtained assuming distance modulus to LMC 18.5 mag [10]. The error of ± 0.05 mag translates to $\pm 7\%$ uncertainty in stellar mass. Lines shown in Figures 2 and 3 were obtained

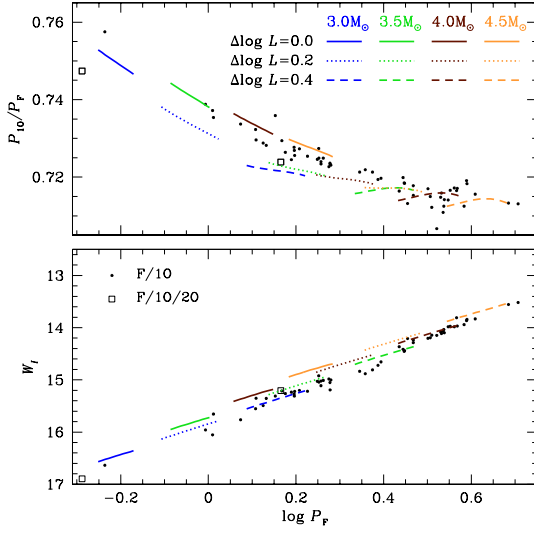


FIGURE 2. Data (points) on the F/10 Cepheids. The Petersen diagram (top) and PL relations (bottom) compared with values for selected models of indicated mass (segments). The segments correspond to the simultaneous instability of the F and 10 modes for models of specified mass and luminosity. Luminosity increments $\Delta \log L$ refer to evolutionary models calculated with $\alpha_{\text{ov}} = 0$.

for models calculated with the OP opacity data [11] for the new solar heavy element mixture [12], adopting $Z = 0.006$. We carried linear nonadiabatic calculations of radial modes for deep unfitted envelope models within the relevant temperature range using the code described in [13]. For luminosity, we first used the values obtained from evolutionary models in the first crossing phase, calculated assuming no overshooting. Then, we considered models with luminosity increments $\Delta \log L = 0.2$ and 0.4 to reproduce the whole range of observed parameters. Models with typical overshooting are brighter by $\Delta \log L \approx 0.15$. Those in the second and third crossings are brighter than models in the first crossing by $\Delta \log L \approx 0.25$ (see [14]).

In the lower panels of Figures 2 and 3, we may see that models of constant mass form nearly a single line in the $\log P - W_I$ plane for specified mode and metallicity. In fact, the dependence on metallicity is quite weak. This means that, once we have credible W_I and the LMC distance, we have quite accurate assessment of a Cepheid mass.

The upper panel of Figure 2 shows the classical Petersen diagram. We may see that the measured period ratios are well reproduced with our models. Comparing plots in the two panels, we note certain problem for $\log P_F < 0.3$. Models with masses near $3M_\odot$ are in agreement with the observational PL relation if some luminos-

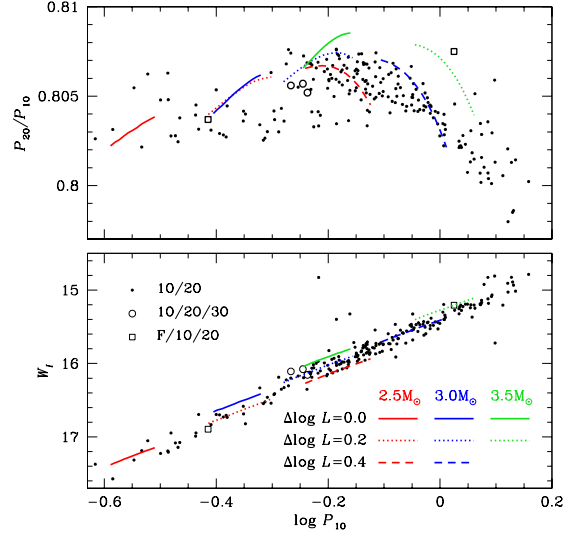


FIGURE 3. The same as Figure 2 but for the 10/20 Cepheids.

ity excess (presumably due to overshooting) is allowed. Thus, the objects may be understood as first crossers. The calculated period ratio is somewhat low. The agreement would improve by choosing lower Z value (see [8]). For the F/10 Cepheids with $\log P_F > 0.3$, both the period ratios and the Wesenheit indexes, point to masses near $4M_\odot$ and the luminosity excess $\Delta \log L \approx 0.4$. These are presumably helium burning objects.

Figure 3 is from DS, where it was concluded that great majority of the LMC 10/20 Cepheids have masses $M = 3.0 \pm 0.5M_\odot$. The objects with $\log P_{10} < -0.2$ are well explained with post-main sequence stellar models crossing the instability strip for the first time, calculated assuming no or moderate overshooting. For those with longer periods, which constitute the majority of the sample, a significant luminosity excess is needed. Interpretation in terms of first crossing models requires an overlarge overshooting, perhaps connected with fast rotation. The difficulty of this explanation is the short crossing time of the instability strip while the number of the objects showing the luminosity excess is relatively high. If these are helium burning objects then the difficulty is the low inferred mass. Standard evolutionary tracks for stars with $M < 3.5$ and acceptable metallicity do not enter the instability strip in this evolutionary phase.

All five triple-mode Cepheids are most likely first crossing objects. Detailed modeling of two 10/20/30 objects implied masses near $3.3M_\odot$ [6]. The third one has very similar periods and Wesenheit index, hence, must have a similar mass. Models of similar mass and calculated with moderate overshooting well reproduce data on

the two 1O/3O Cepheids. The two F/1O/2O objects occur at very different periods. The one at $\log P_{10} = -0.4$ has mass $M < 3.0M_{\odot}$ and that at $\log P_{10} = 0.03$ has mass $M \approx 3.5M_{\odot}$.

NONRADIAL MODES AND TROUBLESOME PERIOD RATIOS

In the radiative interiors of evolved stars, the Brunt-Väisälä frequency, N , is by orders of magnitude larger than frequencies, ω , of radial modes. This implies that all nonradial modes propagate as high-order gravity waves with radial wave number, k_r , satisfying $rk_r = \sqrt{\ell(\ell+1)} \frac{N}{\omega} \gg 1$. The displacement amplitude is $\xi \propto [C_+ e^{i\Psi} + C_- e^{-i\Psi}] e^{-i\omega t}$ with $\Psi = \int dr k_r$.

Large k_r leads to large radiative losses. Global modes exist as long as $|C_-| \sim |C_+|$, and they are unstable if the driving effects in outer layers are strong enough. However, the wave braking occurring at $k_r |\xi| \approx 1$ may prevent growth of an unstable mode amplitude to observable level. Once it occurs, the reflected wave must be ignored ($|C_-| \approx 0$) and this implies wave energy losses. Only with a resonant energy transfer from a nearby radial mode, detectable amplitude of nonradial modes may be maintained. This mechanism, suggested as an explanation for peaks close to radial mode frequencies in RR Lyrae stars [15], may apply also to Cepheids.

Strong radiative damping in the interior leads to $|C_-| \ll |C_+|$. This again justifies ignoring the reflected wave. At sufficiently high- ℓ , there are well-trapped modes, which, in spite of the wave losses, remain unstable [16], [17]. Due to cancelation of opposite sign contributions, the net light changes resulting from such mode excitation are expected low.

The P_X/P_{10} period ratios are concentrated around 0.6 and 0.62. There are no systematic differences in the positions in the PL diagram between the two groups of the 1O/X Cepheids. Both are well inside the 1O band. No radial mode may account for such period ratios. The closest but still far away is P_{30}/P_{10} , as we may see in Figure 4.

Interpretation in terms of nonradial modes is also difficult. In models constrained by observational data, the only modes within the P_X range which do not suffer from strong damping in the deep interior are F-modes (no nodes outside g-wave propagation zone) of ℓ between 40 and 50. For modes of degrees $\ell > 6$, the light changes arise mainly from geometrical distortion of the surface. Then, for even degree modes, the net light amplitude decreases with ℓ only as $\ell^{-0.5}$. Still the amplitude reduction is large and would require intrinsic pulsation amplitudes of these modes significantly larger than those of the 1O modes. Moreover, we have no explanation for the prefer-

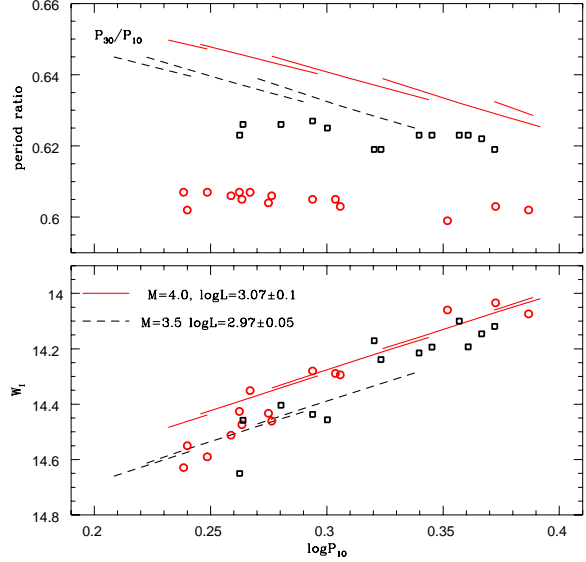


FIGURE 4. Period ratio (top) and Wesenheit indexes (bottom) for 1O/X Cepheids (symbols) compared with calculated values for the 1O/3O Cepheid models (segments). Unfitted envelope models were calculated for temperatures corresponding to the 1O instability range (3O is stable in these models).

ence to 0.6 and 0.62 period ratios.

ACKNOWLEDGMENTS

This work has been supported by the Polish MNiSW grant No 1 P03D 011 30.

REFERENCES

1. I. Soszyński et al., *Acta Astron.*, **58**, 163–185 (2008b).
2. I. Soszyński et al., *Acta Astron.*, **58**, 153–162 (2008a).
3. P. Moskalik, et al., *ASP Conf. Ser.*, **310**, 498–501 (2004).
4. C. Alcock, et al., *Ast. Journ.*, **117**, 920–926 (1999).
5. Y. Alibert, et al., *A&A*, **344**, 551–572 (1999).
6. P. Moskalik and W. A. Dziembowski, *A&A*, **434**, 1077–1084 (2005).
7. J. R. Buchler and R. Szabó, *ApJ*, **660**, 723–731 (2007).
8. J. R. Buchler, *ApJ*, **680**, 1412–1416 (2008).
9. W. A. Dziembowski and R. Smolec, *Acta Astronomica*, **59**, 19–31 (2009).
10. B. E. Schaefer, *Ast. Journ.*, **135**, 112–119 (2008).
11. M. Seaton, *MNRAS*, **362**, L1–L3 (2005).
12. M. Asplund, et al., *A&A*, **417**, 751–768 (2004).
13. R. Smolec and P. Moskalik, *Acta Astronomica*, **58**, 193–232 (2008).
14. A. Pietrinferni, et al., *ApJ*, **612**, 168–190 (2004).
15. W. A. Dziembowski and T. Mizerski, *Acta Astronomica*, **54**, 363–373 (2004).
16. Y. Osaki, *Pub. Astr. Soc. Japan*, **29**, 235–248 (1977).
17. W. A. Dziembowski, *Acta Astron.*, **27**, 95–126 (1977).